A New Superstructure for the $BaAl_4$-Structure Type: An Experimental and Theoretical Study of La_2NiAl_7

Delphine Gout,† Timothy J. Barker, Olivier Gourdon,† and Gordon J. Miller*

Department of Chemistry and Ames Laboratory, U.S. Department of Energy, Iowa State University, Ames, Iowa 50011-3111

Received March 7, 2005. Revised Manuscript Received May 2, 2005

A new ternary aluminide, La_2NiAl_7, has been synthesized from the elements in sealed silica tubes. The crystal structure of La_2NiAl_7 was determined by single-crystal X-ray diffraction and crystallizes in the tetragonal space group *I*4*mm* (No. 123) with $Z = 4$ and lattice parameters $a = 6.221(3)$ and $c = 21.403(2)$ Å. Refinement based on F_0^2 yielded $R_1 = 0.0313$ and $wR_2 = 0.0392$ [$I > 2\sigma(I)$]. It is a new structure type, which belongs to the family of $BaAl_4$-related structures. The La_2NiAl_7 structure corresponds to a 3D superstructure ($\sqrt{2}a \times \sqrt{2}b \times 2c$) of the $BaAl_4$-structure type, whereas La_3Al_{11} is only a 1D superstructure ($3a \times b \times c$). Tight-binding band structure calculations using the density functional theory have been carried out to understand the structural stability of La_2NiAl_7 as well as La_3Al_{11}.

Introduction

Polar intermetallic compounds represent an interesting class of inorganic solids that are intermediate between metallic and nonmetallic *sp*-bonded materials formed by a combination of active, electropositive metals and electronegative metals or semimetals.[1] They are characterized by an optimization of the metal−metal bonding in the electronegative component as determined by a bonding analysis of the electronic density of states: the bonding states are filled and antibonding states are empty, while there is no energy gap at the Fermi level. The active metal behaves like a cation, even if it does not donate its full complement of valence electrons but often provides "lattice stabilization" through cation−anion orbital interactions.[2] Thus, bonding in polar intermetallic compounds is, indeed, intermediate between semiconducting valence compounds (Zintl phases) and *sp*-bonded metallic substances.

In the past few years, exploration of these phases has revealed a wide range of peculiar and novel structures as well as interesting chemical and physical features.[3,4] The most prolific example of this structural class is the tetragonal $BaAl_4$ type (Pearson symbol tI10), whose structure is adopted by hundreds of examples involving transition metals.[5] There are numerous subcategories based on how different elements are arranged: $ThCr_2Si_2$ (*I*4/*mmm*), $CaBe_2Ge_2$ (*P*4/*nmm*), and $BaNiSn_3$ (*I*4*mm*) are three common examples.[6−8] There are also numerous cases showing structures related to the $BaAl_4$-structure type, which involve either superstructures of the basic tetragonal unit cell, as in La_3Al_{11},[9] or intergrowths with other structure types, as in $SrZnBi_2$ ($Sr_{2/2}Zn_2Bi_2/Sr_{2/2}Bi_2$; with InBi type)[10] or $BaCuSn_2$ ($Ba_{2/2}Cu_2Sn_2/Ba_{2/2}Sn_2$; with CrB type).[11] Our research in the La−Ni−Al system has already shown a new structure that is closely related to the $BaAl_4$ type: $LaNi_{1+x}Al_{6-x}$ ($x = 0.44$).[12]

Herein, we report a new compound in the La−Ni−Al system, La_2NiAl_7. Its structure has been determined by both powder and single-crystal X-ray diffraction. This compound exhibits a new 3D superstructure of the $BaAl_4$ type, which originates from an ordering of Ni and Al atoms. The superstructure is unusual as compared to the ones observed in La_3Al_{11},[9] $Ln_3Ni_7As_5$,[13] or $Ce_3Pd_6Sb_3$.[14] In all of these compounds the unit cell is three times larger than the $BaAl_4$-type cell along one direction ($3a \times b \times c$). Moreover, its structure is quite different from the Ba_2AuTl_7 structure that Liu et al. recently found,[15] which is a ternary variant of the orthorhombic $EuIn_4$ type.[16] In this contribution, we also report our investigations of structural stability and bonding properties of La_2NiAl_7 by first-principles calculations and

* To whom correspondence may be addressed. E-mail: gmiller@iastate.edu.
† Current address: Lujan Neutron Scattering Center, Los Alamos National Laboratory, US Department of Energy, MSH805, Los Alamos, NM 87545.

(1) Miller, G. J.; Lee, C.-S.; Choe, W. *Highlights in Inorganic Chemistry*; Meyer, G., Ed.; Wiley-VCH: Heidelberg, 2002; pp 21−54.
(2) Klem, M. T.; Vaughy, J. T.; Harp, J. G.; Corbett, J. D. *Inorg. Chem.* **2001**, *40*, 7020−7026.
(3) (a) Imai, M.; Nishida, K.; Kimura, T.; Kitazawa, H.; Abe, H.; Kito, H.; Yoshii, K. *Physica C* **2002**, *382*, 361−366. (b) Lorenz, B.; Lenzi, J.; Cmaidalka, J.; Meng, R. L.; Sun, Y. Y.; Xue, Y. Y.; Chu, C. W. *Physica C* **2002**, *383*, 191−196.
(4) Gout, D.; Benbow, E.; Gourdon, O.; Miller, G. J. *J. Solid State Chem.* **2003**, *176*, 538−548.
(5) Pearson, W. B. *J. Solid State Chem.* **1984**, *100*, 229−239.
(6) Andress, K. R.; Alberti, E. *Z. Metallkd.* **1935**, *27*, 126−128.
(7) Ban, Z.; Sikirica, M. *Acta Crystallogr.* **1965**, *18*, 594−599.
(8) Eisenmann, B.; May, N.; Müller, W.; Schäfer, H. *Z. Naturforsch.* **1972**, *27b*, 1155−1157.
(9) Gomes de Mesquita, A. H.; Buschow, K. H. J. *Acta Crystallogr.* **1967**, *22* (4), 497−501.
(10) Cordier, G.; Eisenmann, B.; Schaefer, H. *Z. Anorg. Allg. Chem.* **1976**, *426*, 205−214.
(11) Doerrscheidt, W.; Savelsberg, G.; Stoehr, J.; Schaefer, H. *J. Less-Common Met.* **1982**, *83*, 269−278.
(12) Gout, D.; Benbow, E.; Gourdon, O.; Miller, G. J. *Inorg. Chem.* **2004**, *43*, 4604−4609.
(13) Babizhetskyy, V.; Guérin, R.; Isnard, O.; Hiebl, K. *J. Solid State Chem.* **2003**, *172*, 265−276.
(14) Gordon, A.; DiSalvo F. J.; Pöttgen, R. *J. Alloys Compd.* **1995**, *228*, 16−22.
(15) Liu, S.; Corbett, J. D. *Inorg. Chem.* **2004**, *43* (8), 2471−2473.
(16) Fornasini M. L.; Cirafici, S. *Z. Kristallogr.* **1990**, *190*, 295−304.

10.1021/cm050513a CCC: $30.25
Published on Web 06/07/2005

comparison to the hypothetical "$LaAl_4$" structure and the real orthorhombic La_3Al_{11} structure.

Experimental Section

General Synthesis. The title compound was prepared from the elements as obtained (lanthanum ingots, Ames laboratory, 99.99%; nickel powder, Johnson Matthey, 99.997%; aluminum pellets, Aldrich, 99.99%) in the molar ratio La:Ni:Al = 2:1:7. The elements were arc melted under high-purity argon on a water-cooled copper hearth. The weight loss during melting was less than 0.2%. The resulting pellet was annealed at 1073 K in an evacuated silica tube for 10 days. After cooling from 1073 to 673 K for 2 days and, thereafter, a natural cooling to room temperature of the closed furnace, the final product was obtained. Single crystals for La_2NiAl_7 are stable upon exposure to air and water. A microprobe analysis by energy-dispersive X-ray spectroscopy (EDS) performed on a Hitachi S-2460N ESEM gave the chemical formula $La_{2.1(1)}Ni_{0.9(1)}Al_{6.9(3)}$. To obtain the quantitative values, Al, Ni, and La_2O_3 were used as standards.

Crystal-Structure Determination. Silvery block-shaped crystals were selected and mounted in glass capillaries. The crystals were first checked by a rapid scan on a Bruker APEX X-ray diffractometer, and the best crystal was selected for subsequent data collection. All data collections were carried out at room temperature on a Bruker APEX X-ray diffractometer equipped with monochromated Mo Kα radiation. The entire set of reflections was consistent with tetragonal symmetry and could be indexed by a primitive lattice ($a \approx 6.2$ Å and $c \approx 21.4$ Å). The reflection intensities were integrated with the *SAINT* subprogram in the *SMART* Software package.[17] The intensities of the reflections were adjusted for Lorentz polarization and corrected for absorption via a Gaussian analytical method, and the crystal shape and dimensions were optimized with the STOE *X*-Shape program[18] on the basis of equivalent reflections. The *XPREP* subprogram in the *SHELXTL* software package[19] was used for the space group determination, in which systematic absences indicated *I*4/*mmm* and subgroups as possible space groups. At the end of the refinement, the noncentrosymmetric space group *I*4*mm* was chosen because it gave the most satisfactory result. All data treatments, refinements, and Fourier syntheses were carried out with the *JANA2000* program package.[20] The reflection sets were averaged according to the 4/*mmm* point group, yielding internal *R* values of 2.94% for observed reflections ($I > 2\sigma(I)$) (see Table 1 for more information). All refinements were performed on F^2 with all reflections included, but the residual *R* factors are reported for observed reflections only.

A structural model for La_2NiAl_7 was established using direct methods (*SIR97* program[21]). A first series of refinement cycles with isotropic displacement parameters yielded an *R* value of 3.82% (27 parameters). At this stage of the refinement, despite the good *R* value, two atoms labeled initially as aluminum gave negative thermal displacement parameters, which suggest the presence of nickel on those sites. By refinement of these sites as mixed Ni/Al sites, one converges to a full nickel site and the other one to a 50(2)% Ni/50% Al site. These site distributions are in agreement with the measured elemental analysis. Moreover, all the thermal displacement parameters are now positive. Applying anisotropic displacement parameters and a secondary extinction coefficient (type I) led to an *R* value of 3.13% for 49 parameters. Atomic positions, site occupations, and displacement parameters are listed in Table 2. Interatomic distances are listed in Table 3.An X-ray powder diffraction pattern for the sample was measured with a Huber image plate camera, Cu Kα radiation ($\lambda = 1.540562$ Å) to prove the existence of the superstructure that we observed from the X-ray single-crystal experiment. Figure 1 illustrates the powder pattern, and in Table 1 the lattice constants are those given by refinement of the full pattern. These values are used to calculate the interatomic distances listed in Table 3.

Table 1. Structural and Crystallographic Data for La_2NiAl_7

formula weight ($g \cdot mol^{-1}$)	525.38
cryst syst	tetragonal
space group	*I*4*mm* (no.123)
Z	4
cell parameters	$a = b = 6.221(3)$ Å
	$c = 21.403$ (2) Å
volume	828.3(2) Å^3
density calcd ($g \cdot cm^{-3}$)	4.227
temperature	293 K
radiation	$\lambda_{MoK-L2,3} = 0.71069$ Å
diffractometer	Bruker APEX
hkl ranges	$-5 \le h \le 5$
	$-8 \le k \le 27$
	$-27 \le l \le 27$
linear absorption coefficient (mm^{-1})	13.074
absorption correction	analytical
total recorded reflns	3386
obsd reflns ($I > 2\sigma(I)$)	503
R_{int} (%)	2.94
refinement	F^2
weighting scheme	$w = 1/\sigma^2\|F_0\|$
no. refined parameters	49
refinement results	$R(\%) = 3.13/Rw(\%) = 3.92$
	GOF = 1.89
residual electronic density	$[-1.83, +2.01]$ e$^-$/Å^3

Table 2. Fractional Atomic Coordinates and Equivalent Isotropic Atomic Displacement Parameters of La_2NiAl_7

atom	Wyckoff position	x	y	z	B_{eq}[b] (Å^2)
La1	2*a*	1/2	1/2	0	1.07(4)
La2	4*b*	1/2	0	0.25178(9)	1.15(3)
La3	2*a*	0	0	0.00377(9)	1.10(5)
Ni1	2*a*	1/2	1/2	0.1854(3)	1.00(8)
X[a]	4*b*	0	1/2	0.4372(2)	0.74(5)
Al1	2*a*	0	0	0.1915(8)	1.02(3)
Al2	8*c*	0.268(5)	0.268(5)	0.1266(3)	0.84(3)
Al3	8*c*	0.741(3)	0.741(3)	0.3775(3)	0.84(3)
Al4	2*a*	1/2	1/2	0.2975(4)	0.87(3)
Al5	4*b*	0	1/2	0.0519(5)	0.84(3)
Al6	2*a*	0	0	0.3092(5)	0.87(3)

[a] X = 0.50(2)Al/0.50 Ni. [b] $B_{eq} = 8\pi 2/3 \sum_i \sum_j U^{ij} a_i^* a_j^* \mathbf{a}_i \mathbf{a}_j$.

Table 3. Selected Interatomic Distances (Å) in La_2NiAl_7

La−X	3.441(2)
La−Al	3.301(4)−3.582(4)
Ni−Al	2.395(3)
Al−Al	2.568(3)
X−Al	2.461(2)

Structural Discussion

La_2NiAl_7 exhibits a new structure type, which belongs to the family of $BaAl_4$-related structures. A representation of the unit cell is presented in Figure 2. Figure 3 shows the relation between the $BaAl_4$-type unit cell and the one from La_2NiAl_7. The La_2NiAl_7 unit cell is four times larger than

(17) *SMART*, Bruker AXS Inc.: Madison, WI, 1996.
(18) STOE. *X-Shape: Crystal Optimization for Numerical Absorption Correction*; STOE & CIE Gmbh: Darmstadt, Germany, 1996.
(19) *SHELXTL*, version 5.1; Bruker AXS Inc.: Madison, WI, 1998.
(20) Petricek V.; Dusek M. *The crystallographic computing system JANA2000*; Institute of Physics: Praha, Czech Republic, 2000.
(21) Altomare, A.; Cascarano, G.; Giacovazzo, C.; Guagliardi, A.; Moliterni, A. G. G.; Burla, M. C.; Polidori, G.; Camalli, M.; Spagna, R. *SIR97: A package for crystal structure solution by direct methods and refinement*; Italy, 1997.

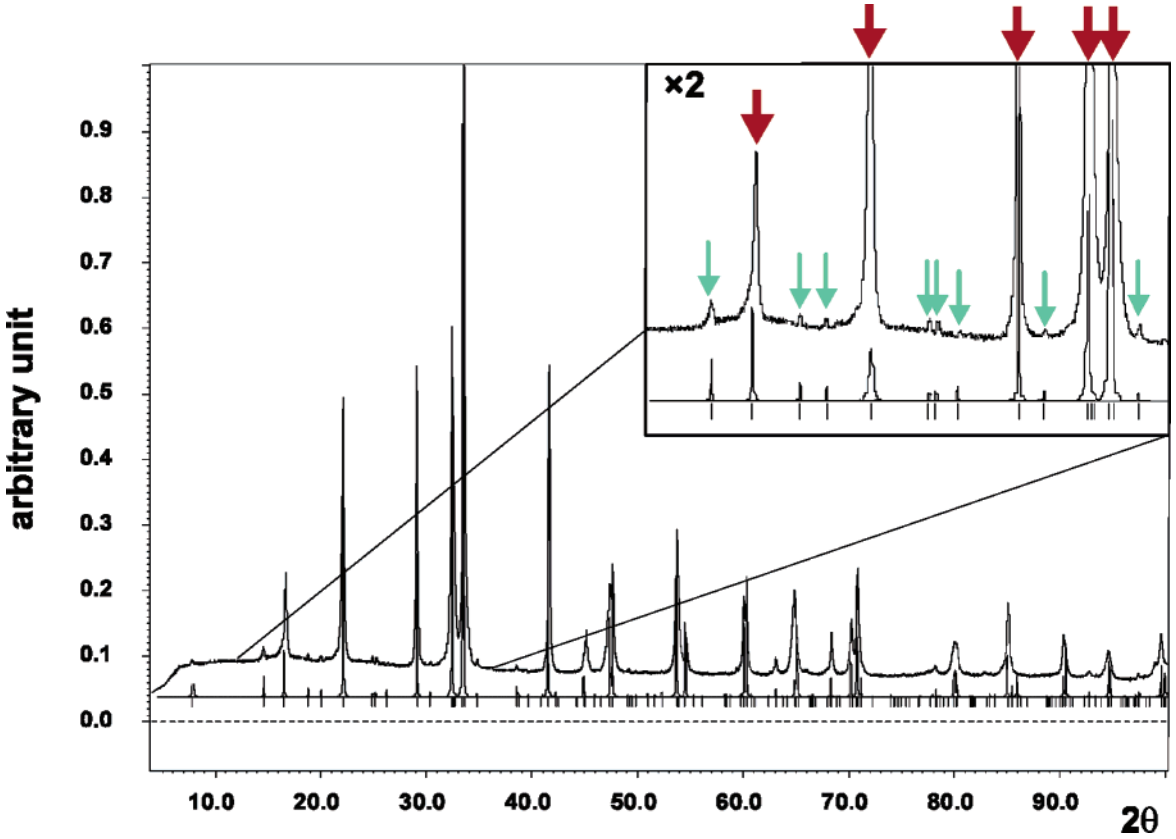

Figure 1. X-ray powder diffraction pattern observed for La_2NiAl_7 together with a calculated pattern. The inset shows an enlarged view (×2) of the angular domain $12 < 2\theta < 35°$. The red arrows indicate the position of the peaks for a regular $BaAl_4$-type structure, whereas the blue arrows indicate the additional peaks of the $\sqrt{2}a \times \sqrt{2}b \times 2c$ superstructure.

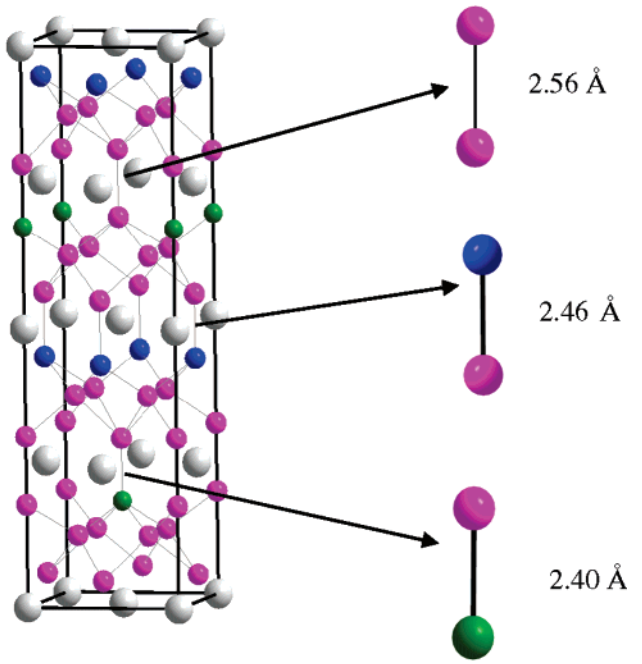

Figure 2. Unit cell of the La_2NiAl_7 structure. The gray, green, blue, and purple spheres correspond, respectively, to the La atoms, Ni atoms, mixed site of Ni/Al atoms, and Al atoms.

the $BaAl_4$ type. As presented in Figure 3 this factor is due to a doubling along the *c* axis as well as a $\sqrt{2} \times \sqrt{2}$ expansion in the *ab* plane, which originates from an ordering of Ni and Al atoms. Indeed, the atomic displacements of these sites are so slight that the difference between the three different dimers is small: Al−Al (2.56 Å), Al−Ni (2.40 Å),

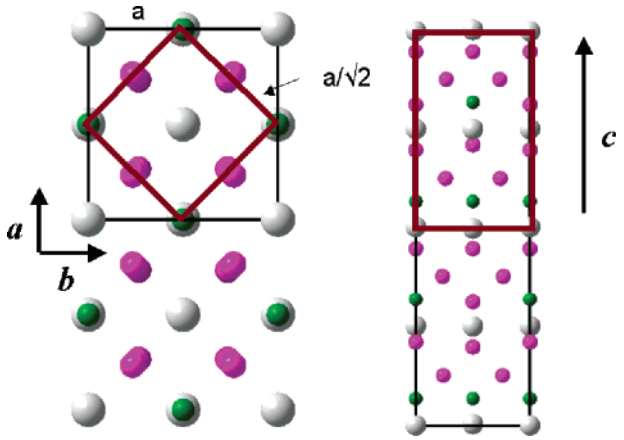

Figure 3. Schematic representation of the $BaAl_4$ superstructure adopted by La_2NiAl_7 (left) in the *ab* plane and (right) along the *c* axis.

and Al−X (2.46 Å). This ordering is quite unusual since many intermetallic rare-earth/nickel/aluminum phases show a disordered situation, as observed for $LaNi_{1.44}Al_{5.56}$,[12] $LaNi_{4.77}Al_{0.23}$,[22] $LaNi_{4.0}Al_{1.0}$,[23] $LaNi_{3.5}Al_{1.5}$,[24] and $CeNi_4Al$.[25] The refined distances in the dimers agree with the nature of the atoms; the Ni−Al distance is shorter than X−Al, which is also shorter than Al−Al. Most of the others interatomic

(22) Xie, C.-M.; Peng, S.-M.; Du, H.-L.; Yao, S.-J.; Shen, W.-D.; Liu, H.-G.; Sun, K.; Chen, B.; Zhang, X.-A.; Liu, L.-J.; Chen, X.-P. *Yuanzineng Kexue Jishu* **2002**, *36*, 447−449.
(23) Achard, J. C.; Givord, F.; Percheron-Guegan, A.; Soubeyroux, J. L.; Tasset, F. *J. Phys.* **1979**, *40*, 218−220.
(24) Dwight, A. E. *Rare Earths Mod. Sci. Tech.* **1978**, 325−330.
(25) Takeshita, T.; Malik, S. K.; Wallace, W. E. *J. Solid State Chem.* **1978**, *23*, 271−274.

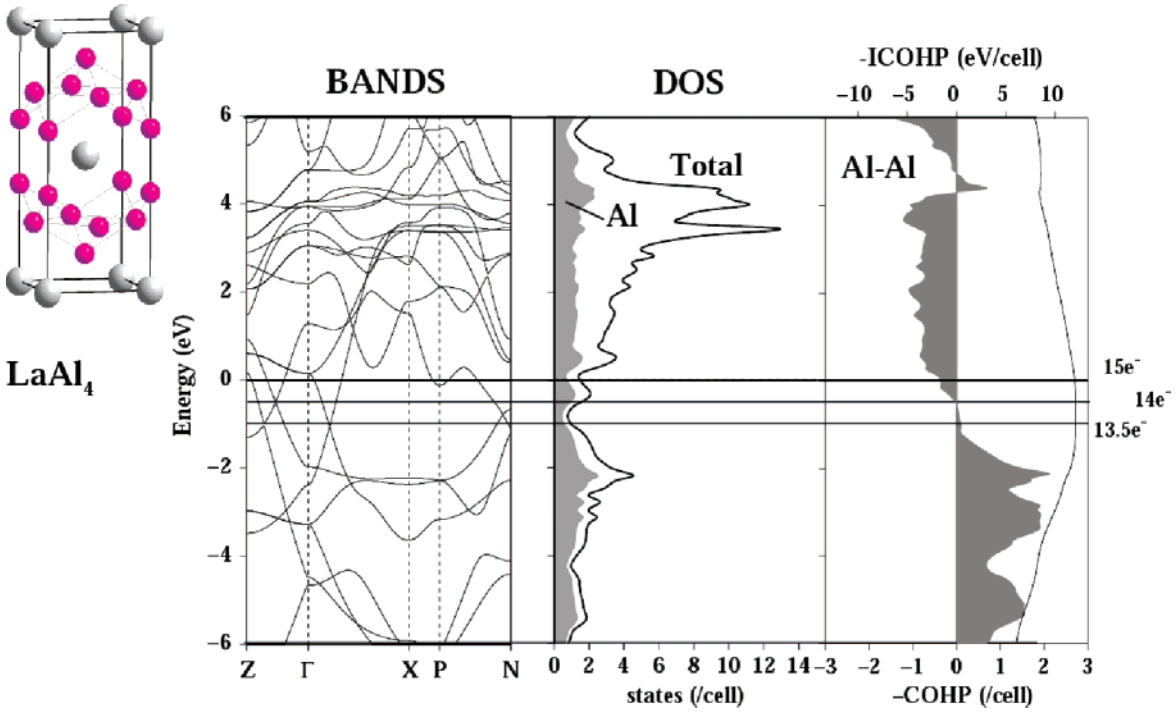

Figure 4. Energy bands along different directions in the first Brillouin zone, DOS and Al−Al COHP with the integrated COHP curve (ICOHP) for the hypothetical "$LaAl_4$" structure with the $BaAl_4$ type. The gray shaded region in the DOS curve is the Al PDOS. Fermi levels for 13.5, 14, and 15 e^- are marked.

distances are in accord with the ones observed in "$LaAl_4$" and are gathered in Table 3.

Other than these specific dimers, the average structure is close to the $BaAl_4$ type as we can see from the X-ray powder pattern in Figure 1. However, the extra peaks relative to the background confirm the superstructure determined from the single-crystal experiment. Superstructures of the $BaAl_4$ type have already been found in other compounds. One of the best examples is La_3Al_{11}, which adopts a unit cell that is three times larger than the parent cell. "$LaAl_4$" is reported only as a high-temperature phase and forms the La_3Al_{11} structure on cooling below 1086(3) K. It is entirely possible that "$LaAl_4$" is truly $LaAl_{3.67}\square_{0.33}$.

Electronic Structure Calculations

To understand the structural stability of this phase, band-structure calculations have been carried out on La_2NiAl_7 as well as on the hypothetical "$LaAl_4$" structure and on the real La_3Al_{11} structure using the tight-binding, linear muffin-tin orbital method (TB-LMTO) with the atomic spheres approximation (ASA).[26] In the TB-LMTO-ASA approach, density-functional theory is used with the local density approximation.[27] Integrations in k space were performed by an improved tetrahedron method[28] on grids of 64 k points within the first Brillouin zone in the case of La_2NiAl_7; 146 k points for $LaAl_4$, and 86 k points for La_3Al_{11}. In our calculations the basis sets included 6s, 5d, and 4f orbitals for La; 4s, 4p, and 3d orbitals for Ni; and 3s and 3p orbitals for Al. The Fermi level was selected as the energy reference. The crystal orbital Hamilton population (COHP) curves,[29] as well as the integrated COHP values (ICOHPs), have been used as additional information about the relative strengths of the different interatomic interactions.

"$LaAl_4$." First, it is instructive to have a closer look at hypothetical "$LaAl_4$" with the $BaAl_4$ type, which corresponds to an average cell and leads to the two superstructures for La_3Al_{11} and La_2NiAl_7. An investigation of the relative stability of La_3Al_{11} and La_2NiAl_7 vs "$LaAl_4$" is the purpose of this theoretical study.

Recently, Amerioun et al. have reported a similar study on the structure and the bonding of Sr_3In_{11}, isostructural to La_3Al_{11}.[30] They emphasize the role of the relative sizes of the component elements to explain the stability of Sr_3In_{11} vs $SrIn_4$. In this work we show that the relative stabilities of La_3Al_{11} and La_2NiAl_7 vs "$LaAl_4$" may be achieved by a certain valence electron count as already pointed out by Liu el al.[15] Figure 4 illustrates the energy bands, the density of states (DOS), and the Al−Al COHP of the hypothetical "$LaAl_4$" in a 12-eV energy window around the Fermi level. The partial DOS (PDOS) of the Al contributions are represented in gray. We identify the Fermi levels for 13.5 e^- ($LaNi_{0.5}Al_{3.5}$), 14 e^- ($LaAl_{3.67}$), and 15 e^- ("$LaAl_4$"); these valence electron counts are based on the numbers of valence s, p, and d electrons of La(3 e^-) and s and p electrons of Ni(0 e^-) and Al(3 e^-). The Ni 3d orbitals lie below −6 eV in the DOS curve and are formally filled with 10 electrons. The DOS curves show that a majority of the La states (La 5d) remain unpopulated, whereas the Al contribution is more pronounced below the Fermi level. The DOS of "$LaAl_4$" has

(26) Andersen, O. K. *Phys. Rev. B* **1986**, *34*, 2439−2449.
(27) Andersen, O. K.; Jepsen, O.; Glotzel, D. In *Highlights of condensed-matter theory*; Bassani, F., Fumi, F., Tosi, M. P., Eds.; New York, North-Holland, Lambrecht, W. R. L., 1985.
(28) Andersen, O. K. *Phys. Rev. B* **1986**, *34*, 2439−2449.
(29) Dronskowski, R.; Blöchl, P. E. *J. Phys. Chem.* **1993**, *97*, 8617−8624.
(30) Amerioun, S.; Häussermann, U. *Inorg. Chem.* **2003**, *42*, 7782−7788.

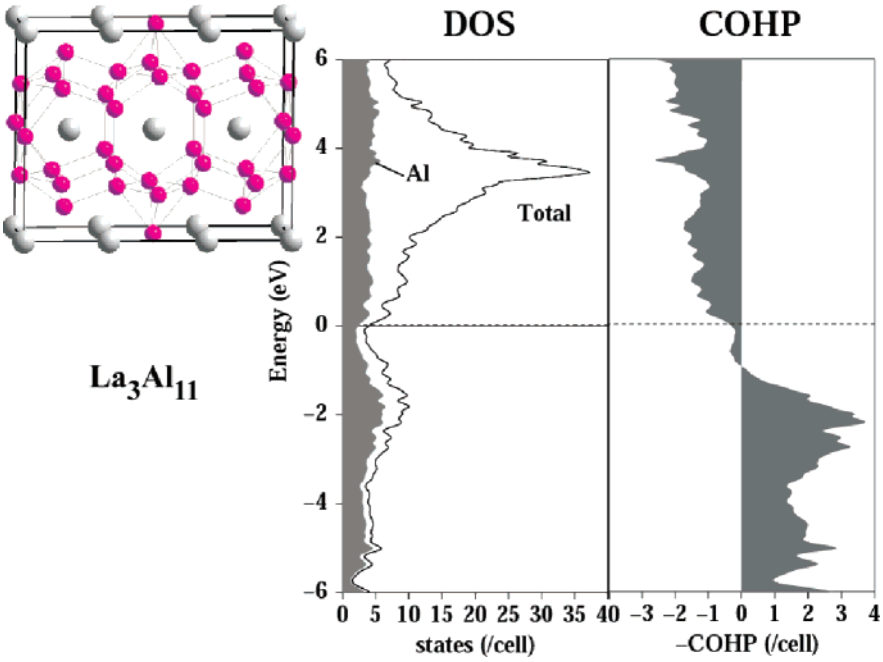

Figure 5. Total DOS with partial DOS from Al and Al−Al COHP curve for La_3Al_{11}.

two low regions of DOS in the vicinity of the Fermi level: one close to 0 eV and the second one around −1 eV. However, according to the Al−Al COHP curve, these minima in the DOS do not correspond to an optimization of the Al−Al bonding as is often seen in other polar intermetallic compounds such as $LaNi_{1.44}Al_{5.56}$.[12] Rather, Al−Al bonding states are fully occupied for 14 valence electrons per formula unit, as seen by several earlier reports.[30−33] For "$LaAl_4$" with 15 valence electrons, Al−Al antibonding states would be occupied. To avoid this electronic situation, nature finds ways to adjust the Fermi level to optimize Al−Al bonding: either (1) by creating vacancies in the structural network as in $LaAl_{3.67}\square_{0.33} = La_3Al_{11}$ or (2) by substituting electron poorer elements for Al as in $LaNi_{0.5}Al_{3.5} = La_2NiAl_7$. Both cases effect depopulating some Al−Al sp-antibonding states and help to stabilize the structure.

For La_2NiAl_7, which corresponds to a formal electron account of 13.5 e^-, we notice that the Al−Al states at this Fermi level are essentially nonbonding states so lowering the electron count slightly below 14 valence electrons will not cost any energy against stabilizing this structure. Indeed, the $BaAl_4$ type is observed for systems between 12 and 14 valence electrons,[34] as in $CaZn_2Al_2$[35] or $LnAu_{1.5}Al_{2.5}$.[36] In the particular cases of La_3Al_{11} and La_2NiAl_7, the Fermi levels at 14 e^- and 13.5 e^-, respectively, correspond to certain band crossing along the ZΓ (**c***) and ΓX (**a*** + **b***) directions in *k* space {Z = (0, 0, $^1/_2$); Γ = (0, 0, 0); and X = ($^1/_2$, $^1/_2$, 0)}. These crossings are possibly an indication of the origin of the superstructures for La_3Al_{11} and La_2NiAl_7.

La_3Al_{11}. The structure of La_3Al_{11} involves "removing" one Al atom at the 4f position in "La_3Al_{12}" and, thereafter, rearranging the remaining Al atoms in the network. This construction disrupts one-third of the Al−Al dimers parallel to the *c* axis in "$LaAl_4$." The remaining Al atoms of the disrupted dimers shift to the midpoint and thus create five-membered rings in the *ac* plane. The resulting DOS and the Al−Al −COHP curve for La_3Al_{11} are shown in Figure 5. The pseudogap at the Fermi level is now pronounced and, based on the COHP analysis, the number of occupied Al−Al antibonding states has diminished. A few Al−Al weakly antibonding states remain occupied and may be explained by the rearrangement of the Al atoms, which have contributed to homogenize the Al−Al distances. Indeed, in La_3Al_{11}, the average Al−Al is approximately 2.75 Å instead of 2.6 Å for "$LaAl_4$." Since there are two distinct La sites, which show coordination environments for both the tetragonal $BaAl_4$ type and the orthorhombic $SrIn_4$ type, the stabilization of the La_3Al_{11} structure is a combination of size and electronic effects.[30] Optimum Al−Al bonding occurs 1 eV below the Fermi level in the DOS for La_3Al_{11}, which suggests that this structure type can accommodate a range of electron counts from ca. 38−42 valence electrons per formula unit. $Ln_3Au_2Al_9$ (Ln = Tb, Dy) are consistent with this conclusion.[37]

La_2NiAl_7. For La_2NiAl_7, the structure retains a complete $BaAl_4$-type network with Ni atoms arranged to eliminate any homoatomic Ni−Ni interactions. Since the observed tetragonal structure has one mixed Ni/Al site (X: 4b), we performed electronic structure calculations on a model with this site fully occupied by Al atoms, which leads to the chemical formula "La_4NiAl_{15}". Figure 6 illustrates the DOS and the Al−Ni and Al−Al COHP curves for this hypothetical compound. With respect to a rigid band model applied to the electronic structure of this structural model, $La_2NiAl_7 = La_4Ni_2Al_{14}$ will have three fewer valence s and p electrons

(31) Liu, S.; Corbett, J. D. *Inorg. Chem.* **2004**, *43* (8), 4988−4993.
(32) Zheng, C.; Hoffmann, R. *Z. Naturforsch. B* **1986**, *41B*, 292−320.
(33) Burdett, J. K.; Miller, G. J. *Chem. Mater.* **1990**, *2*, 12−26.
(34) Häussermann, U.; Amerioun, S.; Eriksson, L.; Lee, C.-S.; Miller, G. J. *J. Am. Chem. Soc.* **2002**, *124*, 4371−4383.
(35) Cordier, G.; Czech, E.; Schäfer, H. *Z. Naturforsch. B* **1984**, *39*, 1629−1632.
(36) (a) Hulliger, F. *J. Alloys Compd.* **1995**, *218*, 255−258. (b) Hulliger, F.; Nissen, H.-U.; Wessichen, R. *J. Alloys Comput.* **1994**, *206*, 263−266.
(37) Nordell, K. J. and Miller, G. J. *Angew. Chem.* **1997**, *109*, 2098−2101.

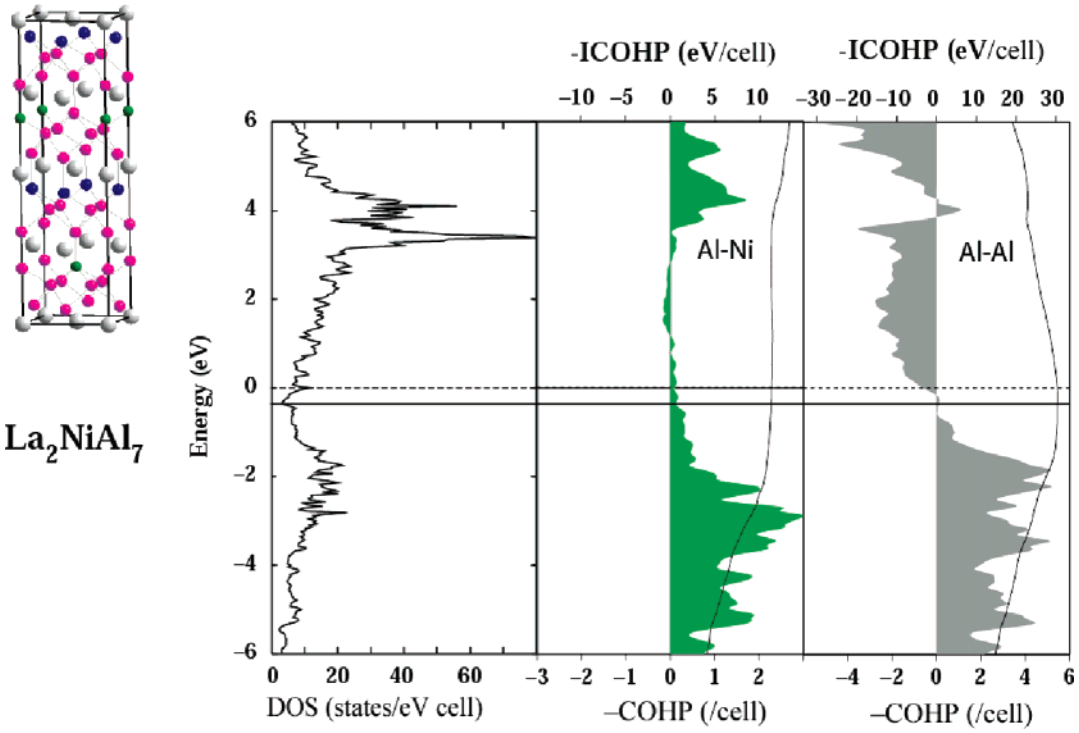

Figure 6. Total DOS, Al−Ni COHP, and Al−Al COHP curves for the hypothetical "La_4NiAl_{15}" (Fermi Level for $La_2Ni_{0.5}Al_{7.5}$ (Dashed Line) and La_2NiAl_7 (Solid Line) Are Marked)

than "La_4NiAl_{15}." These two different electron counts are indicated in Figure 6 by the two different Fermi levels: the one at 0 eV corresponds to the hypothetical "La_4NiAl_{15}", and the one at −0.6 eV corresponds to La_2NiAl_7. Note that the rigid-band Fermi level for La_2NiAl_7 falls in a pseudogap of the DOS. The validity of the rigid band model in this case is due to the complete absence of possible Ni−Ni contacts, which differs from $LaNi_{1.44}Al_{5.56}$.[12] The Ni 3d band lies ca. 2.5 eV below the Fermi level and will be just slightly broadened by increasing the Ni content (the Fermi level will also drop slightly). Furthermore, the Al−Al COHP curve shows full occupation of the Al−Al bonding states for La_2NiAl_7, whereas the Al−Al antibonding states are unpopulated. Indeed, the Fermi level is located in a 0.75 eV wide nonbonding region. In concern of the Al−Ni COHP curve, bonding states remain present up to 1 eV above the Fermi level. However, these states are weakly bonding, essentially nonbonding. Although this curve originates from a calculation on "La_4NiAl_{15}," only subtle changes occur to the shape and features of the curve for La_2NiAl_7, which further validates the rigid band model here.

We also performed a calculation on a hypothetical La_2NiAl_7 compound with the $BaAl_4$-type unit cell in the space group *P*4*mm*, which creates an ordering between Al and Ni atoms in order to satisfy the chemical formulation La_2NiAl_7. However, this hypothetical structure is unstable relative to the observed one by 2.4 eV due to some antibonding Al−Ni states at the Fermi level. Although an optimization of this tetragonal structure, especially of the Al−Ni distance, may result in a comparable energy to the observed superstructure, we have yet to find a more stable arrangement than the one observed by X-ray diffraction.

Magnetic susceptibility measurements show diamagnetic behavior for La_2NiAl_7, which confirms the closed subshell electronic configuration at Ni and discourages the existence of any homoatomic Ni−Ni interactions.

Analogous calculations on Ba_2AuTl_7 not presented in this paper show that its electronic structure is quite different from the one shown in Figure 6 for La_2NiAl_7, although they differ by one valence electron per formula unit. For instance, Corbett et al. have reported that the Tl−Tl bonding states are not totally occupied in Ba_2AuTl_7 but would require two additional valence electrons, which leads to a hypothetical "Ba_2Tl_8."[15] Our TB-LMTO-ASA calculations on Ba_2AuTl_7, which treats the valence functions scalar relativistically, agree with their extended Hückel results. In La_2NiAl_7, the corresponding Al−Al bonding is already optimized. Differences between the DOS of La_2NiAl_7 and Ba_2AuTl_7 can be attributed to a greater s−p splitting in the Au and Tl states than in the Ni and Al states through relativistic contraction of the valence Au and Tl 6s orbitals.

Conclusions

A new polar intermetallic compound in the La−Ni−Al system, La_2NiAl_7, has been synthesized and its structure refined by single-crystal X-ray diffraction. Its structure is a $\sqrt{2}a \times \sqrt{2}b \times 2c$ superstructure of the $BaAl_4$ type, which arises from an ordering of Ni atoms. The observed arrangement precludes any short Ni−Ni contacts in the structure. TB-LMTO-ASA band structure calculations using density functional theory have shown that the parent, hypothetical "$LaAl_4$" needs to reduce Al−Al antibonding interactions and can accomplish this by either creating vacancies, as in La_3Al_{11}, or by substituting more electron-poor elements, such as Ni, as in La_2NiAl_7. In both cases, these calculations have elucidated that the optimization of Al−Al bonding plays a significant role on the relative stabilities of these structures.

The exact nature of the choice of superstructures in these compounds, $3a \times b \times c$ for La_3Al_{11} and $\sqrt{2}a \times \sqrt{2}b \times 2c$ for La_2NiAl_7, still remains an open question. Such studies that include Fermi surface analyses and the study of band crossings in "$LaAl_4$" are currently in progress.

Acknowledgment. This work was supported by NSF DMR 99-81766 and DMR 02-41092. The authors are grateful to Warren Straszheim of the Materials Analysis Research Laboratory of Iowa State University for running energy-dispersive X-ray spectroscopy measurements on our samples and to Dr. Yurij Janssen for magnetization measurements. T.J.B. was supported by NSF 0139152 through the NSF Research Experiences for undergraduate program.

Supporting Information Available: An X-ray crystallographic file in CIF format for the structure determination of La_2NiAl_7. The temperature dependence of magnetization in 0.1 T and the field dependence of magnetization at 1.8 K. This material is available free of charge via the Internet at http://pubs.acs.org.

CM050513A